

Band Gap Engineering of $\text{Cu}_2\text{ZnSnX}_4$ ($X = \text{S, Se and Te}$) Quaternary Semiconductors Using PBE-GGA, TB-mBJ and mBJ+U Potentials

J. Bhavani and Rita John

Abstract—The structural and electronic properties of $\text{Cu}_2\text{ZnSnX}_4$ ($X = \text{S, Se and Te}$) with a tetrahedral coordinated stannite structure have been investigated using first-principles calculations. The optimized lattice constants, anion displacement u , tetragonal distortion parameter η , band gap, density of states and bulk modulus values are reported. The PBE-GGA, modified Becke-Johnson exchange potential (TB-mBJ) and mBJ+U potentials are used to calculate the electronic properties of Cu based quaternary semiconductors $\text{Cu}_2\text{ZnSnX}_4$ ($X = \text{S, Se and Te}$) and thus the results for the band gap and other electronic properties such as Total Density of States (TDOS) and Partial Density of States (PDOS) are analyzed in detail. Also the results obtained using TB-mBJ and mBJ+U potential are compared with the standard local density and Generalized Gradient Approximation (GGA). The comparison shows that the results obtained by TB-mBJ are still underestimating the experimental results. This explains the inadequacy of TB-mBJ potential for semiconductors with strongly delocalized d electrons. Thus in this paper an on-site Coulomb U is incorporated within mBJ potential (mBJ + U) which leads to a better description of the pd hybridization and therefore the band gap which is very much comparable with the experimental results.

Index Terms— $\text{Cu}_2\text{II-IV-VI}_4$ ($X = \text{S, Se and Te}$), band structure, TB-mBJ potential, mBJ+U, Cu-based semiconductor; importance of d-orbitals.

I. INTRODUCTION

Thin film solar cells made of $\text{Cu}(\text{In, Ga})\text{Se}_2$ (CIGS) are increasingly commercialized due to its high efficiency and promising band gaps and compete today as successors of the dominating silicon technology [1], [2]. Due to the increasing price of In and Ga, an alternate to CIGS compounds have been proposed recently. The potential applications of quaternary chalcogenides $\text{Cu}_2\text{ZnSnX}_4$ ($X = \text{S, Se and Te}$) are highly commendable.

These chalcogenide quaternary semiconductor series, $\text{I}_2\text{-II-IV-VI}_4$ are known to have a potential for applications such as photovoltaic absorbers, optoelectronic and thermoelectric materials [3,4]. Among these compounds Cu-based semiconductors $\text{Cu}_2\text{ZnSnX}_4$ ($X = \text{S, Se and Te}$) have optimized band gaps of 1-1.5eV [5-7] and have emerged as promising nontoxic, low-cost and high efficiency material for thin film solar cell applications. Although it is widely

recognized that these multinary semiconductors provide ample opportunities for material design, it is still very difficult to prepare and design high quality quaternary semiconductors because of the substantial uncertainties in determining their crystal structures, electronic, and optical properties. Theoretically, since last two decades, the first principle calculations have been successfully used to design the crystal structure and study its properties. Several hybrid functionals have been proposed, aiming for a better account of the exchange interaction of localized electrons [8]. In order to illustrate the role of Cu d electrons and to explore the importance of group VI anion in determining the band gap, the Full Potential Linearized Augmented Plane Wave (FPLAPW) method with the TB-mBJ potential has been used to investigate the structural and electronic properties of the copper based quaternary compounds in tetragonal stannite (ST) structure (space group 142-m). With the computed optimized lattice constants, the tetragonal distortion $\eta = c/2a \neq 1$ of these semiconductors are calculated which agrees well with theoretical and experimental results (Table I). Knowing the importance of anion displacement the structural properties and the behaviour of $\text{Cu}_2\text{ZnSnX}_4$ ($X = \text{S, Se and Te}$) semiconductors are explored when the group VI anion atoms X (S, Se and Te) are replaced. The total DOS and partial DOS of these compounds are analyzed, as it is essential for the study of the hybridization of the states inside the valence band.

II. METHOD OF CALCULATION

The calculations are performed using FPLAPW within the framework of Density Functional Theory (DFT) [9] using wien2k code [10]. The generalized gradient approximation (GGA) [11] in the scheme of Perdew-Barke-Eruzerhof (PBE), PBE+U, Trans Blaha- modified Becky Johnson (TB-mBJ) [12]-[14] potential and mBJ+U [15] are used. Basis functions were expanded in combination of spherical harmonic functions inside non-overlapping spheres surrounding the atomic sites and by plane waves basis set in the remaining space of the unit cell (interstitial region). The maximal 'lmax' value for the wave function expansion inside the atomic spheres was confined to lmax=10. To achieve the energy eigen value convergence, the wave function in the interstitial region were expanded in plane waves with a cutoff of $k_{\text{max}} = 8/R_{\text{mt}}$, where R_{mt} is the average radius and k_{max} gives the magnitude of the largest k vector in the plane wave expansion. The charge density is Fourier expanded up to $G_{\text{max}} = 12(\text{Ry})^{1/2}$. Self-consistent calculations are considered to be converged when the total

Manuscript received September 4; 2019, revised December 16, 2019.

J. Bhavani is with the Department of Physics, Ethiraj College for Women, Tamilnadu, Chennai, India (e-mail: bhavanishiva24@gmail.com).

Rita John is with Department of Theoretical Physics, University of Madras, Guindy Campus, Tamilnadu, Chennai, India (e-mail: rita.john@unom.ac.in).

energy of the system is stable within 10^{-4} Ry. The integrals over the BZ are performed using 147 k-points in the irreducible BZ. The Cu ($3d^{10} 4s^1$), Zn ($3d^{10} 4s^2$), Sn ($4d^{10} 5s^2 5p^2$), S ($3s^2 3p^4$), Se ($3d^{10} 4s^2 4p^4$) and Te ($4d^{10} 5s^2 5p^4$) orbitals are treated as valence states. The muffin tin radius for Cu, Zn, Sn, S, Se and Te are chosen to be 2.33, 2.36, 2.42, 1.88, 2.17 and 2.37 a.u respectively. There are various empirical methods that estimate the parameter of the screened on-site Coulomb energy (U). However, depending on the fitting procedure, the value of U sometimes varies significantly. For example, the screened Coulomb U for the semicore d electrons in ZnO used in the literature varies from 4.7 to 13 eV [16]. The effective Coulomb U_{eff} is obtained by varying its value from 2eV, 3eV, 4 eV, etc., till the band gap matches with experimental values. The Coulomb U that effectively increases the band gap to the desirable value is considered as U_{eff} . On further variation of Coulomb U, band gap start decreasing. The effective Coulomb energy, $U_{\text{eff}} = U - J$, is about 5.2 eV. For simplicity, we will use this screened Coulomb energy for all the systems to analyze the electronic properties using PBE+U and mBJ+U.

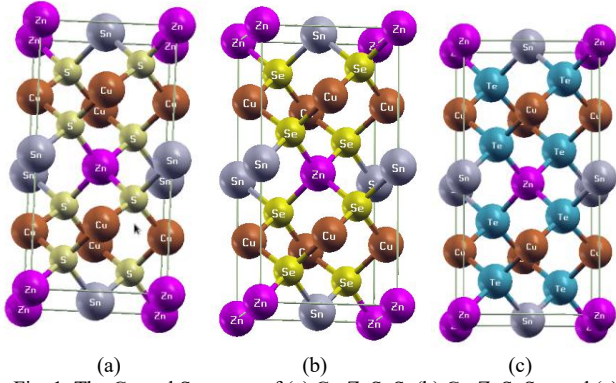


Fig. 1. The Crystal Structure of (a) $\text{Cu}_2\text{ZnSnS}_4$ (b) $\text{Cu}_2\text{ZnSnSe}_4$ and (c) $\text{Cu}_2\text{ZnSnTe}_4$.

III. RESULTS AND DISCUSSION

A. Optimized Structural Properties

The crystal structures of Cu-based quaternary semiconductors are shown in Fig. 1. This structure can be obtained by cation initiation of the group III atoms in ternary semiconductors (I-III-IV₂) to II and IV atoms. The I₂-II-IV-VI₄ quaternary semiconductors have two fundamental crystal structures one is kesterite and other is stannite structure. The structure reported here is stannite structure with a space group I42-m. In all structures, Te or Se or S (group VI) atom is surrounded by two Cu (group I) atoms, one group IV atom (Sn or Ge) and Zn (group II) atom. Therefore the octet rule is obeyed, such tetrahedrally coordinated semiconductors, have three different bonds with group VI atom (Te or Se or S) as center in the stannite structure. The ground state properties of all the three compounds are obtained using the calculations of the total energy (E_{tot}) as a function of volume (V). Fig. 2 shows the E_{tot} versus V curves for $\text{Cu}_2\text{ZnSnX}_4$ ($X = \text{S, Se and Te}$) compounds. These curves were obtained by calculating E_{tot} at several different volumes and by fitting the calculated values to the Murnaghan equation of states.

TABLE I. THE EQUILIBRIUM LATTICE PARAMETERS, a_0 AND c_0 , u , TETRAGONAL DISTORTION η , BULK MODULUS B, ITS PRESSURE DERIVATIVE B' AND VOLUME V_0 OF $\text{Cu}_2\text{ZnSnX}_4$ ($X=\text{S, SE AND TE}$)

Structure	a_0 (Å)	c_0 (Å)	u (Å)	$\eta = c/2a$	B (GPa)	B'	V_0 ($a.u.^3$)
$\text{Cu}_2\text{ZnSnS}_4$	5.487	11.167	0.2433	1.018	70	4.86	1131.27
$\text{Cu}_2\text{ZnSnSe}_4$	5.699	11.831	0.2422	1.038	50	4.48	1309.66
$\text{Cu}_2\text{ZnSnTe}_4$	6.088	12.178	0.2449	1.000	44	5.17	1625.89

TABLE II: THE VALUES OF STRUCTURAL PARAMETERS - η AND u AND BOND LENGTH OF $R_{\text{Cu-VI}}$, $R_{\text{II-IV}}$, $R_{\text{IV-VI}}$ ARE TABULATED

Compound	$\eta = c/2a$	u (Å)	$R_{\text{Cu-VI}}$	$R_{\text{II-IV}}$	$R_{\text{IV-VI}}$
$\text{Cu}_2\text{ZnGeS}_4^{(24)}$	1.003	0.2573	2.3208	5.4162	2.3154
$\text{Cu}_2\text{ZnGeSe}_4^{(24)}$	1.002	0.2539	2.4281	5.6924	2.4189
$\text{Cu}_2\text{ZnGeTe}_4^{(24)}$	1.000	0.2492	2.6119	6.1333	2.7288
$\text{Cu}_2\text{ZnSnS}_4$	1.018	0.2433	2.3451	5.5835	2.4787
$\text{Cu}_2\text{ZnSnSe}_4$	1.038	0.2422	2.4454	5.9155	2.6064
$\text{Cu}_2\text{ZnSnTe}_4$	1.000	0.2349	2.6035	6.0900	2.7062

From the total energy versus volume curves the volume corresponding to the lowest energy is used to determine the zero - pressure equilibrium lattice constant (a_0), the bulk modulus (B_0) and the pressure derivative of the bulk modulus (B'). The calculated values of lattice constant and bulk modulus are presented in Table I. The anion displacement parameter and the $c/2a$ ratio are also optimized for all the compounds. The calculated structural parameter $c/2a$ is more than unity for $\text{Cu}_2\text{ZnSnX}_4$ (S, Se and Te) but the experimental results show that it is less than unity [17]. This discrepancy between theoretical and experimental calculations is due to the fact that the similarity of Cu^+ and Zn^{2+} atoms leads to the cation shift in their experimental structures [18]. Even using X-ray diffraction, it is not easy to detect the cation disorder because only the Zn^{2+} and Cu^+ site ordering is different but both elements have the same X-ray form factor [19]. Partial cation disorder has been observed in $\text{Cu}_2\text{ZnSnS}_4$ sample by neutron diffraction measurement [20]. The strong dependence of the variation of bond lengths as the anion atomic number changes from S to Se to Te is shown in the Table II. Our previous work on $\text{Cu}_2\text{ZnGeX}_4$ ($X = \text{S, Se and Te}$) results are also given for comparison in Table II and 3 [21]. As already discussed, each anion atom in the crystal structure of $\text{Cu}_2\text{ZnSnX}_4$ maintains tetrahedron coordination with two group I atoms, one group IV and one group VI atom.

Also as suggested by Abrahams and Bernstein, for ternary ABC_2 type semiconductors, the group IV elements tend to conserve the tetrahedral bond angles and as a consequence, the bond length between A and C atoms is longer than that between B and C atoms [22]. However it is interesting to note, the bond alteration is in such a way that $R_{\text{IV-V}}$ is longer than $R_{\text{Cu-VI}}$ in $\text{Cu}_2\text{ZnGeTe}_4$ and $\text{Cu}_2\text{ZnSnX}_4$ ($X = \text{S, Se and Te}$) as seen in Table II.

This change over is reflected in the bond alteration parameter u of these compounds where u is less than 0.25 in compounds with $R_{\text{IV-V}} > R_{\text{Cu-VI}}$ and more than 0.25 when $R_{\text{IV-V}} < R_{\text{Cu-VI}}$.

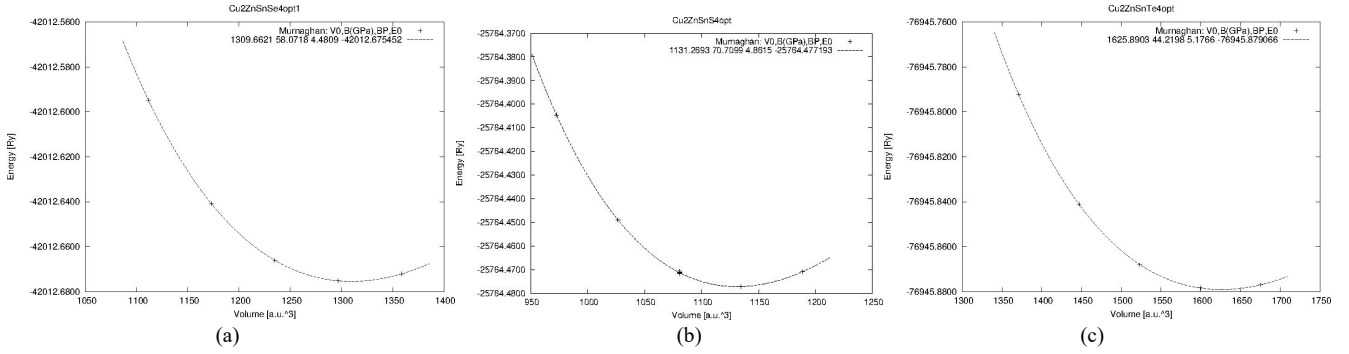
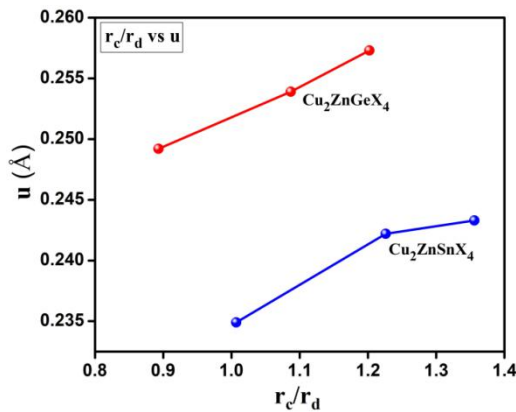

 Fig. 2. Calculated total energy for reduced and extended volume for (a) Cu₂ZnSnS₄ (b) Cu₂ZnSnSe₄ and (c) Cu₂ZnSnTe₄.

Table III shows the linear dependence of the calculated anion displacement u and the ratios of the radius of group IV and group VI anion atoms (S, Se and Te) with the calculated band gap of Cu₂ZnGeX₄ and Cu₂ZnSnX₄ (X = S, Se and Te) compounds. The linear decrease of both u and band gap is evident when radius ratio decreases as the anion varies from S to Se to Te. But with the variation of group IV element from Ge to Sn, u decreases with the increase of its respective radius ratio. Here also u maintains its earlier trend with band gap. The linear relationship between u and radius ratio are shown in Fig. 3.

 TABLE III: RELATION BETWEEN RADIUS OF ATOMS, ANION DISPLACEMENT u AND BAND GAP

Compound	r_c (Å)	r_d (Å)	r_c/r_d	u (Å)
Cu ₂ ZnGeS ₄ ^(*)	1.75	1.46	1.202	0.2573
Cu ₂ ZnGeSe ₄ ^(*)	1.75	1.61	1.087	0.2539
Cu ₂ ZnGeTe ₄ ^(*)	1.75	1.96	0.893	0.2492
Cu ₂ ZnSnS ₄	1.97	1.46	1.356	0.2433
Cu ₂ ZnSnSe ₄	1.97	1.61	1.226	0.2422
Cu ₂ ZnSnTe ₄	1.97	1.96	1.007	0.2349


 Fig. 3. u vs radius ratio of Cu₂ZnGeX₄ and Cu₂ZnSnX₄ (X = S, Se and Te).

B. Electronic Properties

1) Band structure

The band structures of Cu₂ZnSnX₄ (S, Se and Te) are calculated along high symmetry points of the first Brillouin Zone using PBE-GGA, TB-mBJ and mBJ+U potentials are shown in the Fig. 5. The total and partial DOS are calculated using PBE, TB-mBJ and mBJ+U potentials. All three compounds Cu₂ZnSnX₄ (X = S, Se and Te) have direct band gaps with the valence band maximum (VBM) and

conduction band minimum (CBM) located at the same Γ point (Fig. 5). The structural and electronic properties of Cu₂ZnSnX₄ are explained and compared with that of Cu₂ZnGeX₄. The electronic band structure of Cu₂ZnSnX₄ are generic in nature. PBE functional gives a semimetal like band structure whereas gap opens up while using TB-mBJ and mBJ+U. No gap exists between the top most valence band and the lowest conduction band. The band gap of Cu₂ZnSnX₄ (X = S, Se and Te) using Tb-mBJ are found to be 1.263 eV, 1.008 eV and 0.819 eV respectively and the band gap using mBJ+U are 1.418 eV, 1.108 eV and 1.024 eV respectively. Calculated band gap values are compared with other theoretical and the experimental reported values [23], [25] in Table IV. The calculated energy band gap using mBJ+U are much closer to the experimental results than that with PBE-GGA and TB-mBJ. It is because of the fact that the local or semi local functionals (or potentials) underestimate the binding energy of Cu d states and their localization, resulting in an incorrect description of the pd hybridization between Cu d states and anion p states. Hence, while applying an on-site coulomb interaction U , the position of Cu d states are better predicted and hence better describe the pd hybridization. It is observed that mBJ+U potential causes a rigid displacement of the conduction bands towards higher energies with respect to the top of the valence band with small differences in the dispersion at the same regions of the Brillouin zone. Thus reproducing, in general, the characteristic behaviour of the bands [26]. The band structures using TB-mBJ potential does not exactly reproduce the characteristic behaviour of quaternary semiconductors. For example, for all the compounds the electron density is found to be maximum in the second valence bands leaving a larger heteropolar gap between the valence bands. This trend is mainly found in Cu₂ZnSnS₄ and Cu₂ZnSnSe₄ compounds. The compound Cu₂ZnSnTe₄ gives the dispersion of orbitals in both first and second valence bands.

The zero of energy is set to $\Gamma_{4v}^{(2)}$ valence band maximum (VBM). Fig. 5 (using mBJ+U) shows that for all three-compounds there are three distinct VB regions between the VBM and -15.0 eV, separated by two heteropolar gaps. Table V provides the energies of all VB and CB critical points respectively using mBJ+U potential. The upper valence band has its maximum at the $\Gamma_{4v}^{(2)}$ point in the zone center; the conduction-band minimum is at the Γ_{1c} point, hence all three compounds have a direct band gap. There are two secondary maxima in the upper valence band located at $N_{1v}^{(6)}$ and $P_{3v} + P_{4v}$. The minima of upper valence band are

located between $N_{1v}^{(5)}$ and $P_{4v} + P_{5v}$. The width of the first valence band is given by $W_1 = \varepsilon(\Gamma_{4v}^{(2)}) - \varepsilon(N_{1v}^{(5)})$. The width of the first valence band for $\text{Cu}_2\text{ZnSnX}_4$ ($X = \text{S, Se and Te}$) is 5.28 eV, 5.2 eV and 5.1 eV respectively. From Table V it is seen that the width of sulfides is larger than that of selenides and tellurides [27], [28]. The upper valence band is separated by small heteropolar gap from the intermediate valence band. The first heteropolar gap occurs between $N_{1v}^{(5)}$ and $\Gamma_{1v}^{(2)}$. The first heteropolar gap is smallest for $\text{Cu}_2\text{ZnSnS}_4$ (0.67 eV) and it is largest for $\text{Cu}_2\text{ZnSnTe}_4$ (1.60 eV). The width of intermediate band is given by $W_2 = \varepsilon(\Gamma_{1v}^{(2)}) - \varepsilon(\Gamma_{2v})$ and it is narrowest for $\text{Cu}_2\text{ZnSnTe}_4$ semiconductor. The width of the intermediate band for $\text{Cu}_2\text{ZnSnX}_4$ ($X = \text{S, Se and Te}$) is 1.25 eV, 1.04 eV and 0.70 eV respectively. Here also the width of sulfides is larger than the selenides and tellurides. The intermediate band is separated from the lower most valence band by the second heteropolar gap. The second heteropolar band occurs between Γ_{2v} and Γ_{3v} , which is smallest for $\text{Cu}_2\text{ZnSnTe}_4$ (4.05 eV) and largest for $\text{Cu}_2\text{ZnSnS}_4$ (5.6 eV). For $\text{Cu}_2\text{ZnSnSe}_4$ it is 5.26 eV. The lower most valence band occurs between the energy range -12.5 to -14.0 eV between the points $\Gamma_{1v}^{(1)}$ and Γ_{3v} for all three $\text{Cu}_2\text{ZnSnX}_4$ ($X = \text{S, Se and Te}$) compounds. The zero of energy is considered at Γ_{1c} conduction band minimum (CBM). As a general observation, all gaps (band gap and heteropolar gaps) decreases with the increasing molecular weight in the S to Se to Te series, that the gap of sulfides are larger than the gaps of the selenides and tellurides. By comparing the other schemes with mBJ+U functional, the band structures mainly show variation in the occupancy of three different valence bands. Thus the orbital contribution to the VB and CB varies. For example, the upper most valence band (UMV) at Γ occupies the region between (0 to -8.5 eV) and (0 to -5.3eV) for PBE-GGA and mBJ+U respectively for the compound $\text{Cu}_2\text{ZnSnS}_4$. The width of UMV band using PBE-GGA is larger than mBJ+U scheme. The width of UMV band for TB-mBJ is very small ranging from 0 to -0.6 eV. It indicates strong hybridization between the Cu d states and S p states in this region, which is seen in the partial DOS shown in Fig. 7. The tendency of energy range of UMV band is similar for other two compounds.

TABLE IV: COMPARISON OF CALCULATED GGA BAND GAP, CORRECTED BAND GAP USING TB-mBJ AND mBJ+U WITH OTHER AVAILABLE THEORETICAL AND EXPERIMENTAL BAND GAPS

Compound	E_g PBE+U (eV)	E_g TB-mBJ (eV)	E_g mBJ+U (eV)	E_g (exp) (eV)	E_g (th) (eV)
$\text{Cu}_2\text{ZnSnS}_4$	0.43	1.26	1.418	1.50 ⁽³⁴⁾	1.46 ⁽⁷⁾ 1.45 ⁽⁴⁾
$\text{Cu}_2\text{ZnSnSe}_4$	0.40	1.00	1.108	1.15 ⁽³⁴⁾	1.110 ⁽⁷⁾ 1.11 ⁽⁴⁾
$\text{Cu}_2\text{ZnSnTe}_4$	0.28	0.81	1.024	-	-

By comparing the band gap values of $\text{Cu}_2\text{ZnGeX}_4$ and $\text{Cu}_2\text{ZnSnX}_4$ ($X = \text{S, Se and Te}$), it is found that, when a group IV cation atomic number increases from Ge to Sn the band gap value decreases. For example the band gap of $\text{Cu}_2\text{ZnGeS}_4$ is 2.34 eV compared to 1.418 eV of $\text{Cu}_2\text{ZnSnS}_4$.

As the size of Sn is larger than Ge, the anion (VI group) is pushed away from Sn leading to the increase in bond length between IV and VI group atoms as shown in Table II. Therefore from anion displacement equation for ST structure, it is clear that u parameter is larger for $\text{Cu}_2\text{ZnGeX}_4$ compared to $\text{Cu}_2\text{ZnSnX}_4$ thus band gap depends strongly on the anion displacement. The anion displacement equation for stannite structure [29] is,

$$u_{\text{st}} = 0.25 + \frac{\left[R_{\text{Cu-VI}}^2 - \frac{(R_{\text{II-IV}}^2 + R_{\text{IV-VI}}^2)}{2} \right]}{a^2}$$

TABLE V: CALCULATED VALENCE BAND ENERGIES AT HIGH SYMMETRY POINTS (IN eV), RELATIVE TO $\Gamma_{4v}^{(2)}$, Γ_{1c} - VALENCE BAND MAXIMUM AND CONDUCTION BAND MINIMUM OF $\text{Cu}_2\text{ZnSnX}_4$ ($X = \text{S, SE AND TE}$).

State	$\text{Cu}_2\text{ZnSnS}_4$	$\text{Cu}_2\text{ZnSnSe}_4$	$\text{Cu}_2\text{ZnSnTe}_4$
Upper VB			
Maxima			
$\Gamma_{4v}^{(2)}$	0.0	0.0	0.0
$N_{1v}^{(6)}$	0.28	0.30	0.38
$P_{3v} + P_{4v}$	-0.32	-0.35	-0.36
Minima			
$\Gamma_{4v}^{(1)}$	-5.0	-4.85	-4.8
$N_{1v}^{(5)}$	-5.28	-5.2	-5.1
$P_{4v} + P_{5v}$	-5.3	-5.25	-5.18
Intermediate VB			
$\Gamma_{1v}^{(2)}$	-5.95	-6.20	-6.70
Γ_{2v}	-7.2	-7.24	7.4
$N_{1v}^{(4)}$	-6.05	-6.28	-6.85
$N_{1v}^{(3)}$	-7.18	-7.18	-7.23
$P_{1v+2v}^{(2)}$	-6.1	-6.2	-6.9
$P_{5v}^{(2)}$	-7.2	-7.06	-7.38
Lowermost VB			
Γ_{3v}	-12.8	-12.5	-11.45
$\Gamma_{1v}^{(1)}$	-14.08	-13.6	-13.45
$N_{1v}^{(2)}$	-13.0	-12.7	-11.0
$N_{1v}^{(1)}$	-13.45	-13.08	-11.7
$P_{1v+2v}^{(1)}$	-13.0	-12.65	-10.8
$P_{5v}^{(1)}$	-13.5	-12.9	-11.7
Conduction Band			
Γ_{1c}	0.0	0.0	0.0
Γ_{3c}	1.68	1.712	1.596
Γ_{2c}	2.98	2.832	2.076
$N_{1c}^{(1)}$	0.102	0.028	0.0
$N_{1c}^{(2)}$	2.48	2.192	1.976
$P_{1c} + P_{2c}$	1.84	1.90	1.276
P_{5c}	0.6	0.6	0.376

This change in atom displacement sensitively influences the electronic properties of the VBM and CBM and hence leads to the variation of band gap. It is to be noted that the band gap decreases with the increasing anion atomic numbers, i.e., the band gap is 1.418 eV for $\text{Cu}_2\text{ZnSnS}_4$

compared to 1.108 eV for $\text{Cu}_2\text{ZnSnSe}_4$ and 1.024 eV for structure $\text{Cu}_2\text{ZnSnTe}_4$. Similarly the band structure of $\text{Cu}_2\text{ZnGeX}_4$ (X=S, Se and Te) show similar band gap variation.

2) Density of states

Total DOS together with partial DOS using PBE-GGA, TB-mBJ and mBJ+U potentials for $\text{Cu}_2\text{ZnSnX}_4$ (X = S, Se and Te) are computed and the results are compared and analyzed. The results obtained using PBE-GGA and mBJ+U potentials reveal the generic nature of the band structures and density of states of all three compounds and it is confirmed from other experimental results for Cu based quaternary semiconductors. The TDOS of $\text{Cu}_2\text{ZnSnX}_4$ (X = S, Se and Te) using mBJ+U are shown in the Fig. 6. The results show the significance of pd hybridization between Cu d states and anion p states. The band gap of $\text{Cu}_2\text{ZnSnX}_4$ decreases linearly when replacing S with Se and Te. The reduction in the energy gap is not expected as Se is more electronegative than S, which should result in the larger band gap. However the influence of electronegativity is considerably smaller than the influence of p-d hybridization, as explained by Jaffe *et al.*, [30], [31]. The degree of pd hybridization between the Cu-d states and anion-p states determine the valence band energies and band offsets in which a good mixing of pd orbitals ensures more Cu d states being located at the valence band edge [28]. This hybridization is mainly controlled by the energy levels of the atomic orbitals of the constituents, and changing bond length directly affect this degree of hybridization. Therefore by replacing the anion atoms from S to Se and Te, the anion displacement parameter shows considerable variations. This change in the structure plays a predominant role in determining the valence band energies. This is evident from the band structures of $\text{Cu}_2\text{ZnSnX}_4$ compounds (Fig. 5), as more Cu d states are located in the valence band edge when the anion atom changes from S to Se to Te. In the present study the displacement of anion leading to larger bond lengths between group IV and group VI atoms for telluride when compared with selenides and sulfide (Table II). As a direct consequence the increasing bond length lead to decreasing bonding interactions and a subsequent reduction in the band gaps in these quaternary chalcopyrites. Similar observation has been reported by us in II-IV-V₂ pnictides [32], [33].

As discussed in the band structures of $\text{Cu}_2\text{ZnSnX}_4$, the valence band of all the three compounds consist of three main subbands. Here mainly the contribution of individual orbitals using PBE-GGA, TB-mBJ and mBJ+U potential for $\text{Cu}_2\text{ZnSnTe}_4$ compound are analyzed since other two compounds follow same pattern of orbital contribution. For $\text{Cu}_2\text{ZnSnTe}_4$, (Fig. 7), the upper valence band (UVB) is predominantly from Cu 3d states mixed with p states of anion atoms. Following Yamasaki *et al.* [34], the degree of hybridization can be defined by the ratio of Cu d states and anion p states within the muffin tin sphere. Based on this, it can be concluded that the hybridization between Cu d and anion p states becomes weak leading to the broadening of peaks. The lesser interaction between Cu d and Te p states, results in lower band gaps when the group VI atom changes from S to Te. It is observed that this band shifts to lower energy when the anion atomic number increases from S to

Te. This reveals the influence of anion displacement parameter u over the energy gap of any compound as already discussed in the structural properties. The graph drawn between u and band gap obtained using PBE-GGA, TB-mBJ and mBJ+U. The linear relation between u and E_g is shown in the Fig. 4.

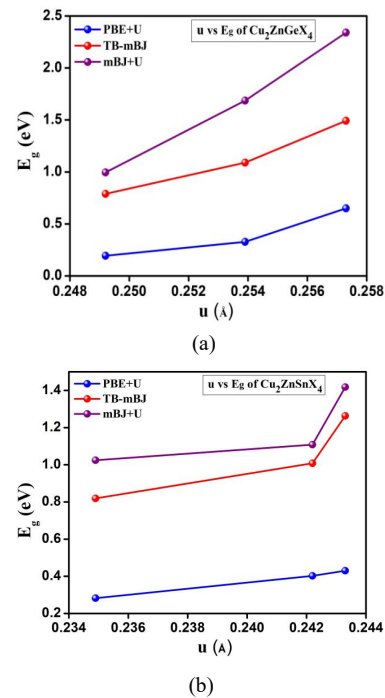


Fig. 4. The linear relation between u and E_g of (a) $\text{Cu}_2\text{ZnGeX}_4$ and (b) $\text{Cu}_2\text{ZnSnX}_4$ (X = S, Se and Te).

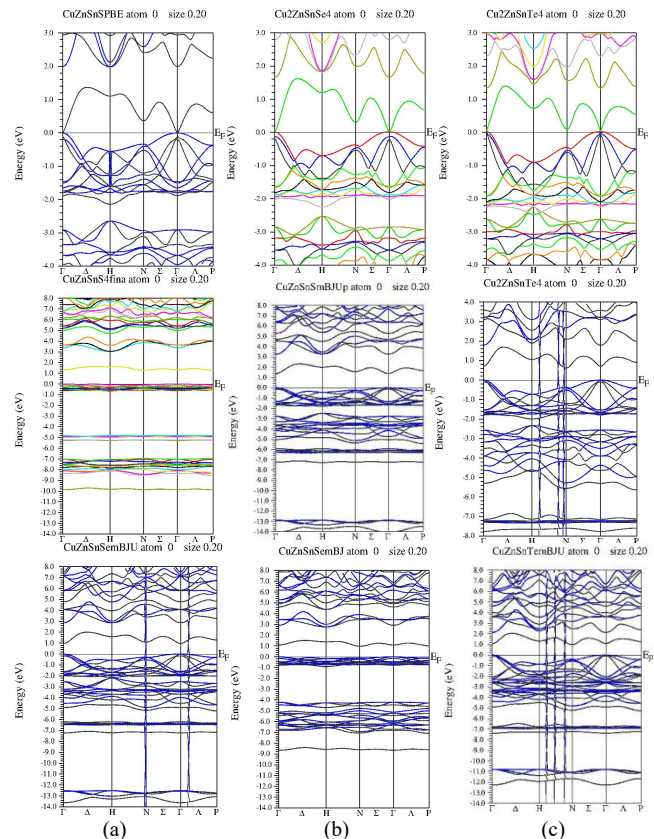


Fig. 5. Calculated band structures along the high symmetry lines in the first Brillouin zone for (a) $\text{Cu}_2\text{ZnSnS}_4$ (b) $\text{Cu}_2\text{ZnSnSe}_4$ and (c) $\text{Cu}_2\text{ZnSnTe}_4$ using PBE-GGA, TB-mBJ and mBJ+U potential respectively.

The second band represents the strong overlapping of bonds from group I orbitals with II group atoms orbitals and

group IV d orbitals with group VI p orbitals. The second valence band region is mainly comprised of S 3p states hybridized with Cu 3d state. Some traces of Sn p orbitals are also seen in this region. The third band is mainly due to the hybridization of anion s & p states with other group II and IV orbitals. In $\text{Cu}_2\text{ZnSnX}_4$ the lowest conduction band is a single band and it is derived from the Sn 4s and anion p states. On applying the on-site potential U , it is observed that in the conduction band the Zn s states are seen completely detached from Zn p states whereas for TB-mBJ potential the overlapping of Zn s and p states are observed. This indicates the strong interaction of orbitals in the upper most valence band that pushes the Zn p orbitals to the higher energy region. The higher conduction bands do not contribute to the band gap values. It is observed that, the broadening of peaks between the energy range of valence and conduction band in TDOS and PDOS for all the three compounds reveals the Same characteristics are also found in $\text{Cu}_2\text{ZnGeX}_4$ compound also. Analyzing the band structure together with the DOS it is observed that the conduction band shifts to the lower energy when the anion atomic number increases from S to Te. These band structures have similar nature as those reported by other journal papers (Table IV) and the internal structure of all the valence bands taken as a group is in fairly good agreement with experiments.

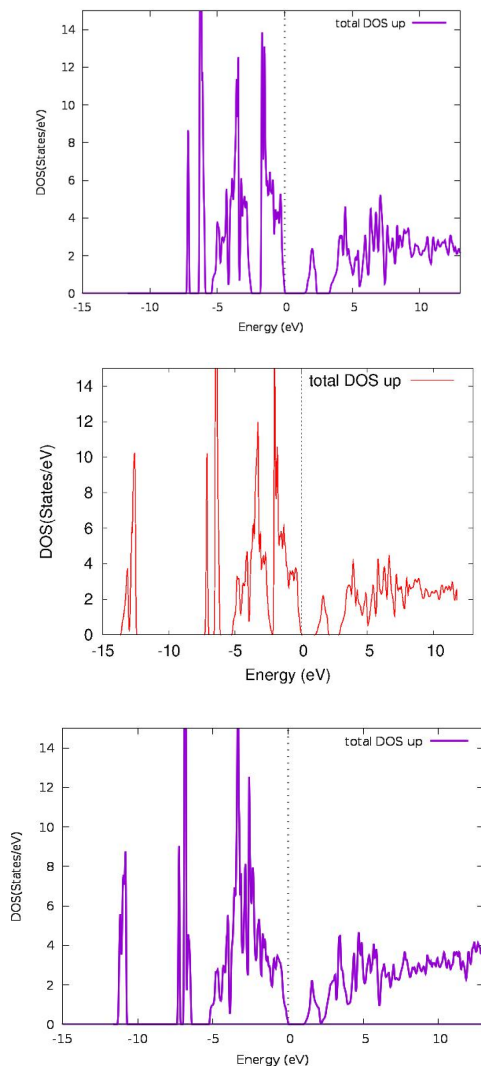


Fig. 6. TDOS using mBJ+U potential for $\text{Cu}_2\text{ZnSnX}_4$ (X = S, Se and Te).

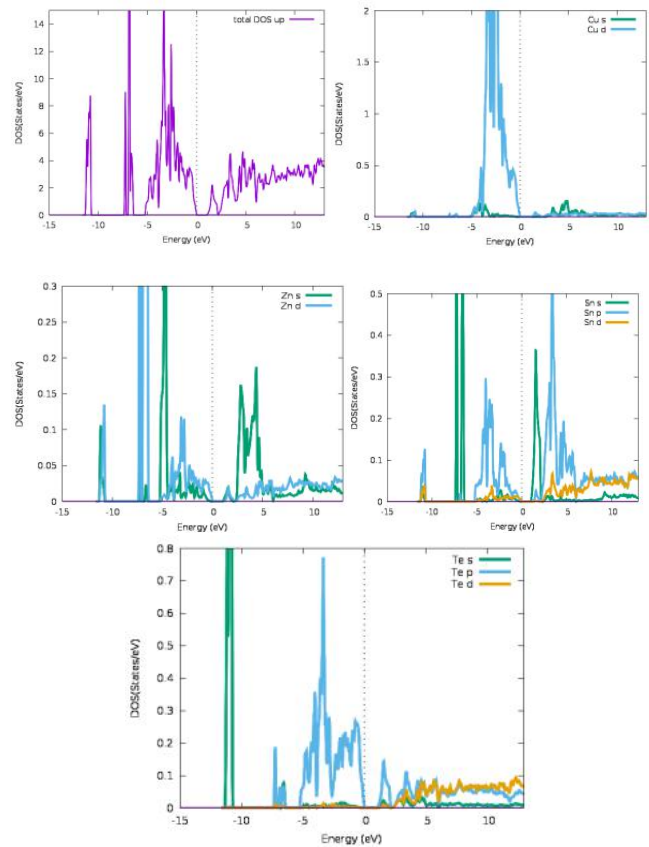


Fig. 7. TDOS and PDOS for $\text{Cu}_2\text{ZnSnTe}_4$ compound using mBJ+U potential.

IV. CONCLUSION

In summary, we have investigated systematically the equilibrium structural properties and electronic band structure of $\text{Cu}_2\text{ZnSnX}_4$ (X=S, Se and Te) quaternary compounds using PBE-GGA, TB-mBJ and mBJ+U exchange potential implemented in wien2k. Both volume optimization and position optimization are carried out. From the optimized lattice constants, the tetragonal distortion parameter η is calculated which agrees well with experimental values. We pointed out that Cu 3d electrons have relatively shallow energy and can hybridize with VI p electrons to form strong covalent bonds. We find that the conduction band shifts downward (lesser band gap) when the group VI anion atomic number increases from S Se Te. i.e, compound with Te shows lesser band gap when compared with Se and S. Also the strong dependence of anion displacement parameter in determining the electronic properties are analyzed. The significance of pd hybridization between Cu d states and anion p states are investigated and presented. A good agreement between our calculated results and experimental data has been obtained. The calculated results show that the energy gaps are substantially improved by mBJ+U over TB-mBJ and PBE-GGA. As a future scope, the method of calculating effective screened Coulomb energy U_{eff} can be extended to other quaternary semiconductors series also. Thus electronic, optical and thermoelectric properties for quaternary compounds can be investigated effectively.

CONFLICT STATEMENT

The manuscript "Band Gap Engineering of $\text{Cu}_2\text{ZnSnX}_4$

(X = S, Se and Te) Quaternary Semiconductors Using PBE-GGA, TB-mBJ and mBJ+U Potentials” is the original research work pursued by us. There is no conflict in this manuscript, we shall be grateful if you could kindly publish the same in your journal.

AUTHOR CONTRIBUTIONS

In my paper only two authors and one is myself and Dr. Rita John is the corresponding author and my Ph.D guide. Both of us did combined analysis and contributed equally. Since I don't have any specific work to differentiate I didn't include in the paper.

REFERENCES

[1] U. P. Singh and S. P. Patra, “Progress in polycrystalline thin film Cu(In,Ga) Se₂ solar cells,” *International Journal of Photoenergy*, Article ID 468147, p. 19, 2010.

[2] S. Rao, A. Morankar, H. Verma, and P. Goswami, “Emerging photovoltaics: Organic, copper zinc tin sulphide, and perovskite-based solar cells,” *Journal of Applied Chemistry*, Article ID 3971579, p. 12, 2016.

[3] S. Schorr, H. J. Hoebler, and M. Tovar, “A neutron diffraction study of the stannite-kesterite solid solution series,” *Enr. J. Mineral.*, vol. 19, p. 65, 2009.

[4] A. Ghosh, R. Thangavel, and M. Rajagopalan, “First principles study of electronic and optical properties of Cu₂ZnSnX₄ (X S, Se) solar absorbers by Tran–Blaha modified Becke–Johnson potential approach,” *J Mater Sci.*, issue 23, vol. 48, pp. 8259-8267, 2013.

[5] A. Shavel, J. Arbiol, and A. Cabot, “Synthesis of Quaternary Chalcogenide Nanocrystals: Stannite Cu₂Zn_xSn_ySe_{1+x+2y},” *J. Am. Chem. Soc.*, vol. 132, p. 4514, 2010.

[6] D. G. Chen and N. M. Ravindra, “Electronic and optical properties of Cu₂ZnGeX₄(X= S,Se and Te) quaternary semiconductors,” *J. Alloys Comp.*, vol. 579, pp. 468–472, 2013.

[7] A. Ghosh, R. Thangavel, and M. Rajagopalan, “First principles study of electronic and optical properties of Cu₂ZnSnX₄ (X S, Se) solar absorbers by Tran–Blaha modified Becke–Johnson potential approach,” *J Mater Sci.*, issue 23, vol. 48, pp. 8259-8267, 2013.

[8] S. Botti, D. Kammerlander, and M. Marques, “Band structures of Cu₂ZnSnS₄ and Cu₂ZnSnSe₄ from many-body methods,” *Applied Physics Letters*, vol. 98, 2011.

[9] F. Tran, P. Blaha, and K. Schwarz, “Band gap calculations with Becke–Johnson exchange potential,” *J. of Physics: Cond. Matter.*, vol. 19, p. 196208, 2007.

[10] P. Hohenberg and W. Kohn, “Density functional theory (DFT),” *Phys. Rev.*, vol. 136, p. B864, 1964.

[11] J. A. Camargo-Martinez and R. Baquero, “The band gap problem: The accuracy of the Wien2k code confronted,” *Revista Mexicana de Fisica*, vol. 59, pp. 453-459, 2013.

[12] X. Ma, Y. Wu, Y. Lv, and Y. Zhu, “Correlation effects on lattice relaxation and electronic structure of ZnO within the GGA+U formalism,” *The Journal of Physical Chemistry C*, vol. 117, no. 49, pp. 26029-26039, 2013.

[13] J. P. Perdew, S. Burke, and M. Ernzerhof, *Phys. Rev. Lett.*, vol. 77, no. 3865, 1996.

[14] A. D. Becke and J. Chem, “A new mixing of Hartree–Fock and local density functional theories,” *Phys.*, vol. 98, p. 1372, 1993.

[15] K. Doverspike, K. Dwight, and A. Wold, “Preparation and characterization of copper zinc germanium sulfide selenide Cu₂ZnGeS_{4-y}Se_y,” *Chem. Mater.*, vol. 2, p. 194, 1989.

[16] A. Bernard, A. Thomas, and B. Fabien, “Screened coulomb interaction calculations: CRPA implementation and applications to dynamical screening and self-consistency in uranium dioxide and cerium,” *Physical Review B*, vol. 89, p. 125110, 2014.

[17] S. Z. Karazhanov, P. Ravindran, A. Kjekshus, H. Fjellvag, U. Grossner, and B. G. Svensson, “Coulomb correlation effects in zinc monochalcogenides,” *J. Appl. Phys.*, vol. 100, p. 043709, 2006.

[18] B.-C. Shih, Y. B. Zhang, W. Q. Zhang, and P. H. Zhang, “Screened Coulomb interaction of localized electrons in solids from first principles,” *Phys. Rev. B*, vol. 85, p. 045132, 2012.

[19] X. Ma, Y. Wu, Y. Lv, and Y. Zhu, 2013, “Correlation effects on lattice relaxation and electronic structure of ZnO within the GGA+U formalism,” *The Journal of Physical Chemistry C*, vol. 117, no. 49, pp. 26029–26039.

[20] R. John, “Influence of structural parameters to engineer the band gaps in ternary pnictides semiconductors – theory as a tool,” *Solid State Phenomena Vols.*, pp. 57-60, 2007.

[21] B.-C. Shih, Y. Zhang, W. Zhang, and P. Zhang, “Screened coulomb interaction of localized electrons in solids from first principles,” *Phys. Rev. B*, vol. 85, p. 045132, 2012.

[22] B.-C. Shih, T. A. Abtew, X. Yuan, W. Zhang, and P. Zhang, “Screened Coulomb interactions of localized electrons in transition metals and transition-metal oxides,” *Phys. Rev. B*, vol. 86, p. 165124, 2012.

[23] S. Schorr, H. J. Hoebler, and M. Tovar, “A neutron diffraction study of the stannite-kesterite solid solution series,” *Eur. J. Mineral.*, vol. 19, no. 65, 2009.

[24] J. Bhavani and R. John, “Band gap engineering of Cu₂-II-IV-VI₄ quaternary semiconductors using PBE-GGA, TB-mBJ and mBJ+U potentials,” *International Journal of Scientific Research in Physics and Applied Sciences*, vol. 7, issue 1, pp. 65-75, February 2019.

[25] F. Tran and P. Blaha, “Accurate band gaps of semiconductors and insulators with a semilocal exchange-correlation potential,” *Phys. Rev. Lett.*, vol. 102, p. 226401, 2009.

[26] B.-C. Shih, Y. B. Zhang, W. Q. Zhang, and P. H. Zhang, “Screened Coulomb interaction of localized electrons in solids from first principles,” *Phys. Rev. B*, vol. 85, p. 045132, 2012.

[27] Y. W. Li, Q. F. Han, T. W. Kim, and W. Z. Shi, “Synthesis of wurtzite–zinblende Cu₂ZnSnS₄ and Cu₂ZnSnSe₄ nanocrystals: Insight into the structural selection of quaternary and ternary compounds influenced by binary nuclei,” *Nanoscale*, vol. 6, no. 3777-3785, 2014

[28] A. Soni, P. Kumar, U. Ahuja, and J. Sahariya, “Structure dependent electronic and optical properties of Cu₂ZnGeX₄ (X=S, Se) solar cell compounds,” *Optik*, p. 62279, 2019.

[29] J. E. Jaffe and A. Zunger, “Electronic structure of the ternary pnictides semiconductors ZnSiP₂, ZnGeP₂, ZnSnP₂, ZnSiAs, and MgSiP₂,” *Phys. Rev. B*, vol. 30, p. 24308, 1984.

[30] F. E. H. Hassan and B. Amrani, “Structural, electronic and thermodynamic properties of magnesium chalcogenide ternary alloys,” *J. Phys.: Condens. Matter*, vol. 19, p. 386234, 2007.

[31] J. E. Jaffe and A. Zunger, “Anion displacements and the band-gap anomaly in ternary ABC₂ chalcopyrite semiconductors,” *Phys. Rev. B*, vol. 27, p. 5176, 1983.

[32] R. John, “Investigation on some of the salient features of II–IV–V₂ pnictides using band structure calculations as a tool,” *Computational Material Science*, vol. 44, pp. 106-110, 2008.

[33] C. Persson, “Electronic and optical properties of Cu₂ZnSnS₄ and Cu₂ZnSnSe₄,” *Journal of Applied Physics*, vol. 107, p. 053710, 2010.

[34] T. Yamasaki, N. Suzuki, and K. Motizuki, “Electronic structure of intercalated transition-metal dichalcogenides: M_xTiS₂ (M = Fe, Cr),” *J. Phys. C*, vol. 20, p. 395, 2010.

Copyright © 2020 by the authors. This is an open access article distributed under the Creative Commons Attribution License which permits unrestricted use, distribution, and reproduction in any medium, provided the original work is properly cited ([CC BY 4.0](https://creativecommons.org/licenses/by/4.0/)).



Rita John is a professor and head of the Department of Theoretical Physics, University of Madras, Chennai, India. She is a Fulbright visiting professor at the Department of Physics and Astronomy, Texas Christian University, Fort Worth, Texas, USA in 2014. She has been teaching solid state physics for graduate students over 20 years. Her area of research is condensed matter physics. She guides Ph.D., M.Phil., M.Sc., and M.Tech. projects. She has over 100 international publications. She is the recipient of various awards and prizes for her academic and research contributions.



J. Bhavani is doing Ph. D under the guidance of Dr. Rita John in the Department of Theoretical Physics, University of Madras, Guindy Campus, Chennai India. She is currently working as an assistant professor in Ethiraj College for Women, Chennai, Tamilnadu, India. Her research work focuses on DFT studies for electronic structure and various properties of quaternary semiconductors.